R. & M. No. 2949
(16,551)
A.R.C. Technical Report

MINISTRY OF SUPPLY

AERONAUTICAL RESEARCH COUNCIL
REPORTS AND MEMORANDA

Some Flutter Tests on Swept-back Wings using Ground-Launched Rockets

By
W. G. MOLYNEUX, B.Sc., and F. RUDDLESDEN, A.M.I.E.I.

LONDON: HER MAJESTY'S STATIONERY OFFICE
1956
PRICE 4s 6d NET

Some Flutter Tests on Swept-back Wings using Ground-Launched Rockets

By

W. G. MOLYNEUX, B.Sc., and F. RUDDLESDEN, A.M.I.E.I.

COMMUNICATED BY THE PRINCIPAL DIRECTOR OF SCIENTIFIC RESEARCH (AIR), MINISTRY OF SUPPLY

Reports and Memoranda No. 2949*

October, 1953

Summary.—This report gives the results of tests on flutter models of untapered wings with 20 deg, 40 deg and 60 deg sweepback. Tests have been made up to a Mach number of $1 \cdot 4$.

A comparison is made between the measured flutter speeds and the speeds estimated using a flutter speed formula. Modifications to the formula are proposed which include a compressibility correction of the form $(1 \cdot 0 - 0 \cdot 166 M \cos \Lambda)$, $0 < M \cos \Lambda < 1 \cdot 6$, where Λ is the angle of sweepback.

A comparison is also made between measured flutter speeds and those calculated using two-dimensional incompressible flow theory. This shows that the calculated speeds are lower than the measured speeds except in the transonic region, where they are in some cases slightly higher. The calculated flutter frequencies are on the average some 20 per cent higher than the measured values.

1. *Introduction.*—The technique of using ground-launched rockets for flutter tests at high Mach number on unswept wings has been described in earlier reports[1]. In the present report tests on untapered wings having 20 deg, 40 deg and 60 deg sweepback at Mach numbers up to $1 \cdot 4$ are described.

The values of flutter speed obtained for these wings are compared with the values estimated using a flutter speed formula[1, 2, 3], and on the basis of this comparison certain modifications to the formula are proposed. A correction to the formula to allow for compressibility effects is proposed in the form of a linear function of the Mach number resolved normal to the wing.

A comparison is also made between the measured values of flutter speed and frequency and the values calculated using two-dimensional incompressible-flow theory and assumed wing modes. The calculated flutter speeds in the transonic region are in come cases slightly higher than those measured, but elsewhere they are lower than the measured values. The calculated flutter frequencies are, in general, greater than the measured values.

Further tests are in progress on wings of delta plan-form, and the application of the flutter speed formula to these wings is to be investigated.

2. *Details of the Models.*—A typical assembly of a swept-back wing on a three-inch diameter rocket is shown in Fig. 1. Both three-inch and five-inch rockets were used for these tests, depending on the predicted flutter speed. With a three-inch rocket the peak speed was about 1,200 ft/sec, Mach number $1 \cdot 07$, and with a five-inch rocket the peak speed was about 2,100 ft/sec, Mach number $1 \cdot 88$.

Wings of 20 deg, 40 deg and 60 deg sweepback were tested. The external dimensions of the wings are given in Table 1 and details of the wing construction are given in Table 2. It may be noted that the wing chord and thickness/chord ratio as measured normal to the axis of sweepback

* R.A.E. Report Structures 155, received 19th March, 1954.

were constant for all the wings. The basic wing structure is shown in Table 2, and consisted of a plywood sheet cut to the wing plan-form, carrying a spar at 30 per cent chord aft of the wing leading edge, a solid wood filler (generally balsa) cut to the required contour, and a plywood nose forward of the 45 per cent chord line. Lead strip, fixed to the plywood sheet, was used to adjust the position of the wing inertia axis, and by varying the spar material the wing stiffness could also be varied.

3. *Test Procedure.*—Static measurements of the inertia and elastic characteristics were made on all the wings. To determine the elastic characteristics the wing was rigidly fixed at the root and measurements were made with loads applied firstly to a wing section in the line of flight at 70 per cent semi-span outboard from the root, and secondly to a wing section normal to the wing at 70 per cent semi-span outboard from the root as measured along the 30 per cent chord line (the line of the wing spar). In each case a pure torque was applied in increments in the plane of the loading section and displacements of the loading section were measured. Values for wing torsional stiffness for the two loading sections were obtained and also the point of zero linear displacement in the loading section under pure torque load (the 'flexural centre'). Values for wing flexural stiffness for the two loading sections were obtained from measurements of displacement of the loading section for a load applied at the flexural centre normal to the plane of the wing. The mean values of torsional and flexural stiffnesses, and flexural centre positions, for port and starboard wings of each model, are given in Table 3.

Resonance tests were made on the wings with fixed root to determine the frequencies and nodal line positions for the first three modes. In general the fundamental mode was mainly flexural, the first overtone was mainly torsional and the second overtone was mainly overtone flexure. The nodal line for the torsion mode of each wing lay at an approximately constant fraction of the chord aft of the leading edge. The resonance frequencies and nodal line positions for all the wings are given in Table 4.

In general no attempt was made to measure the wing modes, but for one 60-deg swept wing (No. 1178) the fundamental and first overtone modes were measured for use in calculations. To obtain the modes pins were inserted at intervals along the wing leading and trailing edges and the amplitudes of vibration of the pin heads were recorded on waxed paper. The amplitudes were then measured using a microscope, and by correlating these measurements with the nodal line locations the appropriate sign could be allocated to the pin displacements. It was apparent that line of flight wing sections were distorting in the overtone mode, but to simplify the calculations the distorted wing chord-line was approximated by a straight line passing through the leading edge of the chord-line and through the nodal point of the section. This 'linearised' mode gave poor agreement with the measured trailing-edge displacement (Fig. 2) but the agreement was worst at the tip and improved for inboard sections. The modes obtained on this basis are the 'measured' modes shown in Fig. 3.

The models, when flutter tested, were in general fitted with one vibration pick-up only However, models 1130, 1131 and 1175 were tested with a pick-up in each wing to determine whether the flutter was symmetric or antisymmetric in character. All models were launched at an elevation of $12\frac{1}{2}$ deg and a continuous photographic record was obtained of the signals from the vibration pick-ups in the wings. The flight path of the model was followed by ciné-cameras and the velocity was measured by radio reflection Doppler equipment. From these records the speed and acceleration of the model at commencement of flutter, the flutter frequency and the speed at which the wings failed were determined. These measurements are given in Table 4.

4. *Flutter-Speed Formula.*—An estimate of wing flutter speeds was obtained from a flutter-speed criterion[1, 2, 3]. The criterion written in the form of a flutter-speed formula is as follows:

$$V = \left(\frac{m_\theta}{\rho_0 S c_m^{\,2}}\right)^{1/2} \frac{(0\cdot 9 - 0\cdot 33K)(1 - 0\cdot 1r)\left(0\cdot 95 + \dfrac{1\cdot 3}{\sigma_w}\right)\sec^{3/2}(\Lambda - \frac{1}{16}\pi)}{0\cdot 854(g - 0\cdot 1)(1\cdot 3 - h)} \quad \ldots \quad \ldots \quad (1)$$

(the symbols are defined in Table 3).

The wing semi-span, s, is used in the formula instead of the distance to the equivalent tip, $d(= 0 \cdot 9s)$, and the numerical constant is accordingly reduced from $0 \cdot 9$ to $0 \cdot 854$. Also, in the above formula a compressibility factor is, for the moment, omitted.

With the exception of the sweepback function all the parameters in the above expression are intended to be determined by assuming the wing to be unswept[2]. This introduces some uncertainties, however, particularly for highly swept wings, because the root constraint is not representative of the unswept wing case. It was decided, therefore, to make speed estimates from the formulae firstly using parameters determined in a manner considered more appropriate for swept wings, and secondly using parameters determined as if the wing were unswept, as originally intended. The associated stiffness measurements were described in section 3. In the first set of estimates the wing stiffnesses were determined with loads applied to a wing section in the line of flight, and dimensions were measured normal to the root or in the direction of flight. In the second set of estimates stiffnesses were determined with loads applied to a wing section normal to the axis of sweepback and dimensions were measured along the axis of sweepback or normal to it. The value of h that was used in the formula was the flexural centre position for the loading section (*see* section 3). The estimates of flutter speeds obtained by these two methods are given in Table 3.

5. *Method of Flutter Calculation.*—A method of calculation based on static stiffness measurements, such as was used for the unswept rocket models[1], could not readily be applied to a swept wing because of the uncertainty in the determination of the appropriate stiffnesses. Instead, a method was used which was based on measured resonance characteristics of the wings and certain assumed modes.

The results of the resonance tests indicated that the wings could be divided into three broad categories characterised by the nodal line of the first overtone mode being at about $0 \cdot 45c$, $0 \cdot 50c$ and $0 \cdot 59c$ respectively (*see* Table 5). These positions were taken as the actual nodal line positions for the wings and were used as the reference axis positions for the flutter calculations. The following assumptions were then made:

(*a*) The fundamental mode could be represented by the combination of a bending mode of the reference axis corresponding to the fundamental bending mode of a uniform cantilever beam with a torsion mode about the reference axis of sections in the line of flight corresponding to the fundamental twisting mode of a uniform cantilever beam

(*b*) The first overtone mode could be represented by a torsion mode about the reference axis of sections in the line of flight, corresponding to the fundamental twisting mode of a uniform cantilever beam.

The amount of torsion present in the fundamental mode was determined by making the cross-inertia coefficient for the fundamental and first overtone modes zero for a wing having the mean values of inertia axis position and radius of gyration given in Table 5. On this basis the ratio of actual cross inertia to the geometric mean of the direct inertias did not exceed $0 \cdot 10$ for any of the wings.

The flutter calculations were made using these assumed fundamental and first overtone modes as the two degrees of freedom. The elastic coefficients for these modes were determined using the measured fundamental flexure and torsion frequencies (n_1 and n_2 in Table 4) and the known inertias. The aerodynamic coefficients were determined using two-dimensional incompressible flow derivatives[4], multiplied by the cosine of the angle of sweepback. The results are given in Table 4.

Calculations were made on one wing (No. 1178) using both these assumed modes and the measured modes, and the results are given in Table 6.

6. *Discussion of Results.*—6.1. *Measured Results.*—The two methods of stiffness measurement give stiffness values which differ considerably (Table 3). In general the flexural stiffness as measured for a line of flight section is less than that measured for a section normal to the sweep

axis, whereas the reverse obtains for the torsional stiffnesses. The difference increases with wing sweepback, and for the 60-deg swept wings the ratio of flexural stiffnesses is about 1 : 4 and the ratio of torsional stiffnesses about 2 : 1. The positions of the flexural centre at the loading sections also differ considerably. With load applied in the line of flight the flexural centre moves forward with sweepback and ranges from about $0 \cdot 25c$ for 20-deg sweep to a position forward of the leading edge at 60-deg sweep. With load applied normal to the sweep axis it moves aft with sweep-back and ranges from about $0 \cdot 40c$ at 20-deg sweep to an extreme position aft of the trailing edge at 60-deg sweep.

The measured wing frequencies are given in Table 4 and it can be seen that in general the first three resonances are reasonably separated in frequency. However, for three of the wings (Nos. 1165, 1131 and 1173) the first and second overtone frequencies are very close together and for wing 1173 the overtone flexural frequency is slightly lower than the torsional frequency. These three wings were constructed of solid balsa with no wing spar (Table 2).

The telemetry records of wing oscillations were of three distinct types:

(*a*) Divergent flutter oscillations leading to wing failure during the rocket acceleration period

(*b*) Intermittent oscillations during the rocket acceleration period with divergent flutter oscillations leading to wing failure during the deceleration period

(*c*) Intermittent oscillations during the rocket acceleration and deceleration periods without wing failure.

Records of type (*b*) were obtained on models 1124, 1144, 1145 and 1166, and records of type (*c*) were obtained on models 1146, 1147, 1150, 1152, 1160, 1161, 1162, 1163 and 1178. It was noted that in records of type (*b*) the frequency of the intermittent oscillations corresponded to that of the final flutter oscillations.

It may be that records of type (*b*) and (*c*) can be explained by the existence of a narrow region of speed for divergent flutter oscillations that is traversed before the flutter can develop to wing failure. With these records the speed at which the intermittent oscillation commenced was taken as the flutter speed, and the frequency of the oscillations was taken as the flutter frequency.

No oscillations were recorded on models 1148, 1149, 1153 and 1154 up to a speed in the region of 2,000 ft/sec. Models 1130, 1131 and 1175, which were fitted with two pick-ups to establish whether symmetric or antisymmetric flutter was obtained, all gave records of symmetric flutter.

Measured flutter speeds and frequencies are given in Table 4. The flutter speeds range from about 600 ft/sec to 1,600 ft/sec and the flutter frequencies from about 20 cycles/sec to 60 cycles/sec. The flutter frequency parameter $2\pi nc/V$ ranges from about $0 \cdot 25$ to $0 \cdot 45$.

6.2. *Speed Estimates from the Flutter-Speed Formula.*—Estimates of flutter speeds using the formula of section 4 are given in Table 3. It can be seen that the speeds estimated from measurements appropriate to a line of flight loading section and from measurements appropriate to a loading section normal to the sweep axis differ considerably and are roughly in the ratio of 1 to 2. This discrepancy can largely be attributed to the term $(1 \cdot 3 - h)$ in the criterion, which is intended to allow for the effect on flutter speed of variation of wing flexural axis position. For an unswept wing the flexural axis position can be measured readily but the same cannot be said for the swept wing. For the present estimates the flexural *centre* position for the loading section has been used as an alternative to flexural *axis* position, but the range of variation of flexural centre position, from $-0 \cdot 23$ to $1 \cdot 13$, is far outside the limits of variation for flexural axis position, from $0 \cdot 2$ to $0 \cdot 4$, which were proposed in the original form of the criterion[4]. However, if the term is omitted from the formula then the flutter speeds obtained by both methods of estimation are practically equal (*see* V_A and V_B in Table 3).

6.2.1. *Comparison of measured and estimated speeds.*—The speed estimates obtained with the term $(1 \cdot 3 - h)$ neglected are in reasonable agreement with the measured speeds. The ratios of measured speed to estimated speed are given in Table 3, and are shown plotted against Mach number resolved normal to the wing in Fig. 5.

Also plotted in this figure are some published results of flutter tests on swept wings in a low-speed wind tunnel[2]. These are included so that trends at low Mach numbers, where the ground-launched rocket method is inapplicable, can be established. The results are shown plotted against the Mach number for the estimated speeds, rather than against the measured Mach number as has been done in earlier work[1]. A compressibility correction to the formula expressed in terms of measured Mach number is useless to a designer using the formula to obtain an estimate of wing flutter speed, and the usual procedure with a correction in this form is to apply it at some arbitrary Mach number, generally that corresponding to the maximum design diving speed of the aircraft. By expressing the compressibility correction as a function of the 'estimated' Mach number the application of the correction becomes straightforward.

The values of V_B for models 1131 and 1173 differ considerably from the measured values. However, the first and second overtone frequencies for these two wings were almost coincident (Table 4) and the formula does not allow for the effect on flutter of a frequency coincidence. The effect is not apparent on the values of V_A for these wings. Also shown on Fig. 5 are curves of the function $(1 - M^2 \cos^2 \Lambda)^{1/4}$, $0 < M \cos \Lambda < 0 \cdot 9$. This function has been suggested as a compressibility correction to the formula for speed estimates for unswept wings[3], and some evidence in support of it has been obtained[1]. The function forms a boundary to the test results for these wings, and if used in this form in the formula it would in general result in an under-estimate of flutter speed. On the other hand the linear function $(1 \cdot 1 - 0 \cdot 2M \cos \Lambda)$, $0 < M \cos \Lambda < 1 \cdot 5$, is a good mean line through the experimental points, and its use in the formula would give an average estimate of flutter speed with a possible error of about $\pm$ 20 per cent on the true value. It is to be noted that the scatter of the experimental points about this mean line is greater for measurements with a line of flight loading section than for measurements with a loading section normal to the axis of sweep.

The above linear form of the compressibility factor implies that there is a compressibility correction at zero Mach number. However, the real significance of this is that even when compressibility effects are negligible the flutter-speed formula provides a speed estimate that, on the average, is some 10 per cent lower than the measured speed. The anomaly can be avoided by reducing the numerical factor in the formula from 0·854 to 0·78, thus increasing the estimated speeds by about 10 per cent, and at the same time reducing the compressibility factor to $(1 \cdot 0 - 0 \cdot 166M \cos \Lambda)$, $0 < M \cos \Lambda < 1 \cdot 6$. In Fig. 6 one set of the swept-wing results have been replotted on this basis together with some results for unswept wings[2], and the proposed linear compressibility factor is seen to represent a good average value for all the wings.

The linear function has three main advantages over the Glauert function. It is easier to apply, it is more closely related to the test results, and from the design viewpoint it involves less penalty on structural stiffness since the compressibility correction is smaller.

On the basis of the present tests it is therefore suggested that the formula should exclude the term involving wing flexural axis position, the numerical constant should be reduced from 0·854 to 0·78, and a compressibility correction of the above linear form should be applied,

i.e.
$$V_1 = \left(\frac{m_0}{\rho_0 s c_m^{\,2}}\right)^{1/2} \frac{(0 \cdot 9 - 0 \cdot 33K)(1 - 0 \cdot 1r)\left(0 \cdot 95 + \dfrac{1 \cdot 3}{\sigma_w}\right) \sec^{3/2} (\Lambda - \frac{1}{16}\pi)}{0 \cdot 78(g - 0 \cdot 1)} \quad \ldots \quad \ldots \quad (1)$$

$$V_E = V_1(1 \cdot 0 - 0 \cdot 166 M_1 \cos \Lambda)\,, \qquad 0 < M_1 \cos \Lambda < 1 \cdot 6 \quad \ldots \quad \ldots \quad \ldots \quad \ldots \quad (2)$$

where V_E is the final estimated flutter speed and M_1 is the free-stream Mach number corresponding to the speed V_1.

The formula can be applied either with measurements appropriate to a loading section in the line of flight or with measurements appropriate to a loading section normal to the axis of sweep.

6.3. *Flutter Calculations*.—The results of the flutter calculations based on assumed modes and two-dimensional incompressible flow derivatives are given in Table 4.

Flutter calculations were made on model 1178 using both assumed and measured modes, and the comparison between the modes is shown in Fig. 3. The fundamental modes are in reasonable agreement, but the same cannot be said of the overtone modes. It can be seen that the torsion component in the assumed overtone mode differs considerably from that measured. However, despite these differences in the modes, the calculated flutter speeds and frequencies are in very close agreement (*see* Table 6). So far as the flutter results are concerned, therefore, there appears to be little difference between calculation using the particular assumed modes chosen and one using measured modes. It is to be noted, also, that using the assumed modes involved considerably less experimental and computational work, since only three sets of coefficients (corresponding to the three reference axis positions at $0 \cdot 45c$, $0 \cdot 50c$ and $0 \cdot 59c$) were needed for the flutter calculations on all the wings.

6.3.1. *Comparison of measured and calculated results*.—The ratios of measured to calculated values of flutter speed and frequency are given in Table 4, and are shown plotted against the measured Mach number, and against the measured Mach number resolved normal to the wing, in Fig. 7. In general the measured flutter speeds are greater than those calculated, but a close agreement of the results is not to be expected since the aerodynamic coefficients used in the calculations do not allow for the effects of either aspect ratio or compressibility. The lower boundary to the tests results shows a slight dip at transonic Mach numbers. This dip shows a minimum at a free-stream Mach number of about $1 \cdot 1$, but when the results are plotted against Mach number resolved normal to the wing the dip is more gradual and a minimum occurs at a resolved Mach number of about $0 \cdot 95$.

The results for one wing of 40-deg sweepback and one of 60-deg sweepback are well below the boundary for the remainder of the results. For both these wings the first and second overtone natural frequencies were in close proximity (*see* Table 4), and to obtain a reliable result a flutter calculation in more than two degrees of freedom would be required.

The calculated flutter frequencies are, in general, greater than those measured, an average value of the ratio of measured : calculated frequency for these wings being about $0 \cdot 8$. However, this frequency ratio is to some extent dependent on the wing sweepback and ranges from an average value of about $0 \cdot 7$ for 20-deg sweepback to about $0 \cdot 9$ for 60-deg sweepback.

7. *Conclusions*.—On the basis of the present tests it is suggested that the formula for the estimation of wing flutter speeds should exclude the term involving wing flexural position and that the numerical constant should be reduced from $0 \cdot 854$ to $0 \cdot 78$. It is also proposed that the factor for compressibility effects should be a linear function of the Mach number as resolved normal to the wing. The proposed modified formula is as follows:

$$V_1 = \left(\frac{m_0}{\rho_0 s c_m^{\,2}}\right)^{1/2} \frac{(0 \cdot 9 - 0 \cdot 33K)(1 - 0 \cdot 1r)\left(0 \cdot 95 + \frac{1 \cdot 3}{\sigma_w}\right) \sec^{3/2}\left(\Lambda - \frac{1}{16}\pi\right)}{0 \cdot 78(g - 0 \cdot 1)}$$

$$V_E = V_1(1 \cdot 0 - 0 \cdot 166 M_1 \cos \Lambda), \qquad 0 < M_1 \cos \Lambda < 1 \cdot 6$$

where V_E is the required flutter speed estimate and M_1 is the free stream Mach number corresponding to the speed V_1. Measurements appropriate to loading sections either in the line of flight or normal to the axis of sweepback may be used.

The fixed root flutter speeds calculated using two-dimensional incompressible-flow theory and assumed wing modes are, in the transonic region, in some cases slightly higher than those measured, but elsewhere they are lower than the measured values. The calculated flutter frequencies are, in general, some 20 per cent greater than the measured values.

Acknowledgement.—Acknowledgements are due to the staff of Guided Weapons Department, Trials Division, for assistance given in the testing of these models.

REFERENCES

No.	Author	Title, etc.
1	W. G. Molyneux, F. Ruddlesden and P. J. Cutt.	Technique for flutter tests using ground-launched rockets, with results for unswept wings. R. & M. 2944. November, 1951.
2	W. G. Molyneux	The flutter of swept and unswept wings with fixed-root conditions. R. & M. 2796. January, 1950.
3	A. R. Collar, E. G. Broadbent and E. B. Puttick	An elaboration of the criterion for wing torsional stiffness. R. & M. 2154. January, 1950.
4	I. T. Minhinnick	Subsonic aerodynamic derivatives for wings and control surfaces. R.A.E. Report Structures 87. A.R.C. 14,228. July, 1950.

TABLE 1

Wing Dimensions

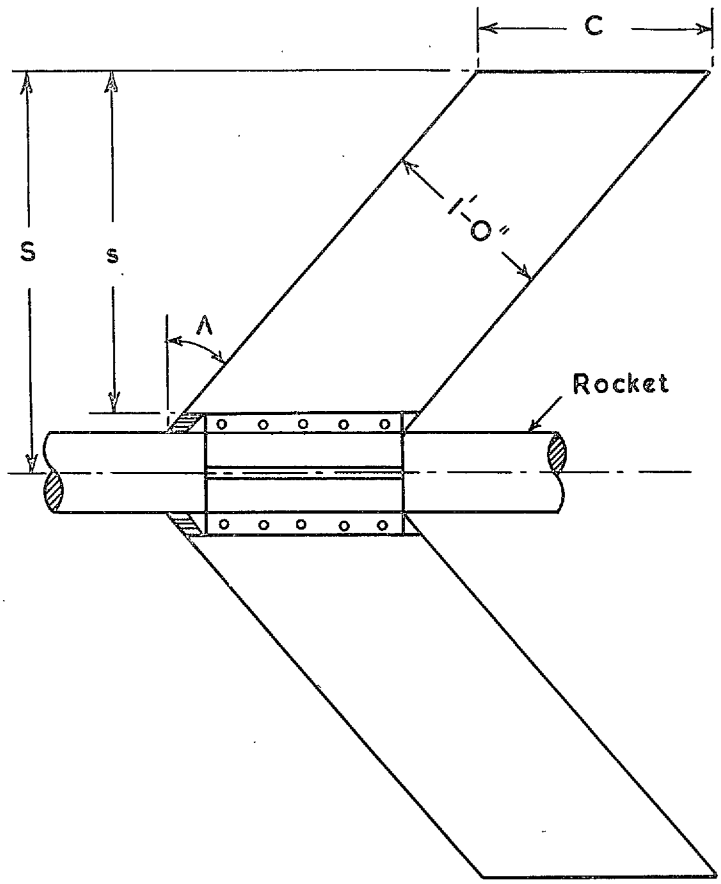

		Angle of Sweepback, Λ		
		20°	40°	60°
Distance from root to tip, s–ft		1·53	1·53	1·53
Wing chord in line of flight, C–ft		1·06	1·31	2·00
Aspect ratio, $\frac{2S}{C}$	3" rocket	3·3	2·7	1·75
	5" rocket	3·4	2·8	1·8
Thickness:chord in line of flight		0·094	0·077	0·050
Wing section		RAE 101	RAE 101	RAE 101

TABLE 2. Details of Wing Construction

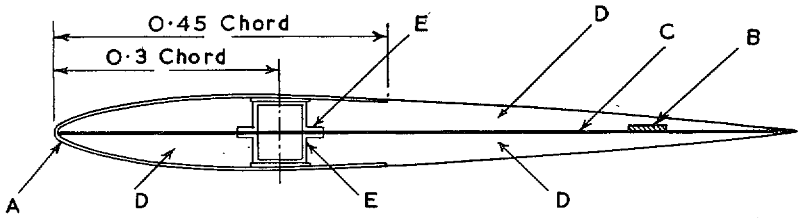

Model No	A	B	C	D	E
1120	—	—	1/8" Plywood	Solid Balsa	—
1124	—		—	Solid Spruce	—
1125		0·39"x 1/16" Lead Strip at 82·25% Chord	1/32" Plywood	Solid Balsa	30 SWG Alclad Box Spar
1129	—	—	1/32" Plywood	Solid Balsa	1/2"x O·6" Solid Spruce Spar
1130	1/32" Plywood	—	1/8" Plywood	Solid Balsa	—
1131	—	—	1/8" Plywood	Solid Balsa	—
1132	—	0·39"x 1/16" Lead Strip at 82·25% Chord	1/32" Plywood	Solid Balsa	30 SWG Alclad Box Spar
1133	—	—	1/8" Plywood	Solid Balsa	1/2"x O·6" Solid Spruce Spar
1144	1/32" Plywood	—	1/8" Plywood	Solid Balsa	24 SWG Alclad Box Spar
1145	1/32" Plywood	—	1/8" Plywood	Solid Balsa	22 SWG Alclad Box Spar
1146	1/32" Plywood	—	1/8" Plywood	Solid Balsa	20 SWG Alclad Box Spar
1147	1/32" Plywood	—	1/8" Plywood	Solid Balsa	18 SWG Alclad Box Spar
1148	1/32" Plywood	—	1/8" Plywood	Solid Balsa	16 SWG Alclad Box Spar
1149	1/32" Plywood	—	1/8" Plywood	Solid Balsa	14 SWG Alclad Box Spar
1150	1/32" Plywood	—	1/8" Plywood	Solid Balsa	24 SWG Alclad Flanged Box Spar
1151	1/32" Plywood	—	1/8" Plywood	Solid Balsa	22 SWG Alclad Flanged Box Spar
1152	1/32" Plywood	—	1/8" Plywood	Solid Balsa	20 SWG Alclad Flanged Box Spar
1153	1/32" Plywood	—	1/8" Plywood	Solid Balsa	18 SWG Alclad Flanged Box Spar
1154	1/32" Plywood	—	1/8" Plywood	Solid Balsa	16 SWG Alclad Flanged Box Spar
1155	1/32" Plywood	—	1/8" Plywood	Solid Balsa	14 SWG Alclad Flanged Box Spar
1160	—	—	1/8" Plywood	Solid Balsa	24 SWG Alclad Box Spar
1161	—	—	1/8" Plywood	Solid Balsa	16 SWG Alclad Box Spar
1162	1/32" Plywood	—	1/8" Plywood	Solid Balsa	24 SWG Alclad Flanged Box Spar
1163	1/32" Plywood	—	1/8" Plywood	Solid Balsa	16 SWG Alclad Flanged Box Spar
1164	—	—	—	Solid Spruce	—
1165	—	—	1/8" Plywood	Solid Balsa	—
1166	1/32" Plywood	—	1/8" Plywood	Solid Balsa	—
1167	—	—	1/8" Plywood	Solid Balsa	O·5"x O·54" Solid Spruce Spar
1168	1/32" Plywood	3/8"x 1/16" Lead Strip at 75% Chord	1/8" Plywood	Solid Balsa	24 SWG Alclad Box Spar
1169	1/32" Plywood	3/8"x 1/16" Lead Strip at 75% Chord	1/8" Plywood	Solid Balsa	16 SWG Alclad Box Spar
1170	1/32" Plywood	3/8"x 1/16" Lead Strip at 75% Chord	1/8" Plywood	Solid Balsa	24 SWG Alclad Flanged Box Spar
1171	1/32" Plywood	3/8"x 1/16" Lead Strip at 75% Chord	1/8" Plywood	Solid Balsa	16 SWG Alclad Flanged Box Spar
1172	—	3/8"x 1/16" Lead Strip at 75% Chord	—	Solid Spruce	—
1173	—	3/8"x 1/16" Lead Strip at 75% Chord	1/8" Plywood	Solid Balsa	—
1174	1/32" Plywood	3/8"x 1/16" Lead Strip at 75% Chord	1/8" Plywood	Solid Balsa	
1175	—	3/8"x 1/16" Lead Strip at 75% Chord	1/8" Plywood	Solid Balsa	1/2"x O·6" Solid Spruce Spar
1178	—		—	Solid Spruce	—

TABLE 3. Comparison of Measured and Estimated Flutter Speeds

Model No.	Λ	g	V_M	Loading Section in Line-of-Flight 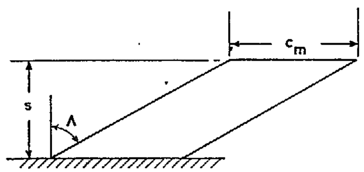							Loading Section Normal to Sweep Axis 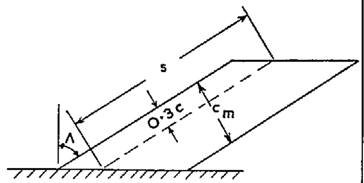							$\frac{V_M}{V_A}$	$\frac{V_M}{V_B}$
				l_ϕ	m_θ	h	$\rho_w G$	V	V_A	M_A	l_ϕ	m_θ	h	$\rho_w G$	V	V_B	M_B		
1120	20°	0·45	675	434	548	0·32	1·3	715	700	0·63	651	439	0·85	1·4	1380	620	0·56	0·96	1·09
1160	20°	0·42	1150	4030	1630	0·27	1·5	1060	1190	1·07	5160	1670	0·66	1·6	1890	1210	1·09	0·97	1·00
1161	20°	0·39	1275	4560	2520	0·11	1·7	1400	1670	1·50	5450	2400	0·44	1·8	1940	1670	1·50	0·77	0·77
1162	20°	0·39	1160	3840	1860	0·25	2·0	1330	1400	1·25	5030	1740	0·41	2·1	1530	1360	1·22	0·83	0·85
1163	20°	0·40	1560	6290	3000	0·23	1·7	1630	1740	1·56	8360	2840	0·39	1·8	1890	1720	1·54	0·90	0·91
1164	20°	0·42	725	2150	615	0·37	1·8	735	682	0·61	2720	585	0·55	1·9	860	644	0·58	1·06	1·13
1165	20°	0·45	—	215	517	0·27	1·3	668	688	0·62	355	340	1·13	1·4	3270	556	0·50	—	—
1166	20°	0·43	930	1560	970	0·20	1·4	837	920	0·82	1650	890	0·49	1·5	1120	915	0·82	1·01	1·02
1167	20°	0·44	575	1280	442	0·28	1·3	563	574	0·51	1670	435	0·46	1·4	685	553	0·50	1·00	1·04
1124	40°	0·42	890	2600	1430	0·28	1·5	1020	1040	0·91	5550	835	0·64	1·9	1490	940	0·84	0·86	0·95
1125	40°	0·47	800	1190	780	0·14	1·0	610	708	0·64	2650	610	0·45	1·3	835	710	0·64	1·13	1·13
1129	40°	0·43	970	2970	1300	0·18	1·0	840	941	0·84	5310	1000	0·44	1·3	1130	990	0·89	1·03	0·98
1130	40°	0·43	1000	1610	1260	0·03	1·2	914	1018	0·91	2830	905	0·61	1·5	1490	1030	0·92	0·98	0·97
1131	40°	0·45	530	138	349	0·03	0·9	434	560	0·50	528	133	1·07	1·2	1610	370	0·33	0·95	1·43
1132	40°	0·47	790	1190	780	0·14	1·0	618	716	0·64	2650	610	0·45	1·3	835	710	0·64	1·10	1·11
1133	40°	0·43	650	990	650	0·26	1·1	689	716	0·64	2170	416	0·60	1·5	970	680	0·61	0·91	0·96
1144	40°	0·41	1125	3090	1720	0·05	1·2	950	1200	1·07	4830	1310	0·50	1·6	1550	1240	1·11	0·94	0·91
1145	40°	0·42	1080	3520	1970	0·05	1·3	990	1240	1·11	5360	1540	0·53	1·7	1670	1290	1·16	0·87	0·84
1146	40°	0·41	1120	3820	2110	0·06	1·3	1060	1320	1·18	5730	1580	0·50	1·7	1700	1360	1·22	0·85	0·82
1147	40°	0·42	1270	3720	1830	0·07	1·4	938	1160	1·04	5430	1780	0·57	1·8	1960	1430	1·28	1·10	0·89
1148	40°	0·40	—	3970	2830	0·03	1·5	1280	1630	1·46	6330	2060	0·42	1·9	1800	1590	1·42	—	—
1149	40°	0·40	—	5870	3220	0·03	1·5	1310	1660	1·49	8950	2950	0·59	2·0	2740	1940	1·74	—	—
1150	40°	0·42	1190	4480	2200	0·11	1·4	1060	1260	1·13	6950	1560	0·47	1·8	1510	1250	1·12	0·94	0·95
1151	40°	0·40	1160	4730	2230	0·10	1·4	1130	1350	1·21	6920	1550	0·47	1·9	1600	1330	1·19	0·86	0·87
1152	40°	0·40	1300	4570	2600	0·08	1·5	1230	1500	1·35	6630	1680	0·51	1·9	1810	1430	1·28	0·87	0·91
1153	40°	0·39	—	6250	2690	0·09	1·5	1230	1490	1·34	9370	1990	0·45	1·9	1810	1540	1·39	—	—
1154	40°	0·39	—	5600	2910	0·07	1·5	1310	1610	1·45	7810	2040	0·50	2·0	2020	1620	1·45	—	—
1155	40°	0·39	780	690	777	0·10	1·6	770	927	0·83	1580	441	0·76	2·0	1460	790	0·71	0·84	0·99
1168	60°	0·45	1020	2130	1670	-0·10	0·9	670	935	0·84	6140	905	0·62	1·8	1700	1010	0·90	1·09	1·01
1169	60°	0·44	1180	2790	2690	-0·04	1·0	965	1290	1·16	9150	1150	0·54	2·0	1550	1305	1·17	0·91	0·90
1170	60°	0·45	1330	3260	2300	0·08	1·0	855	1040	0·93	9070	1280	0·51	2·1	1720	1353	1·21	1·28	0·98
1171	60°	0·42	1580	3960	3040	-0·07	1·1	980	1340	1·20	10430	1520	0·56	2·2	2190	1620	1·45	1·18	0·98
1172	60°	0·47	1135	3950	3260	0·05	0·9	1000	1250	1·12	15580	1200	0·63	1·9	1700	1137	1 02	0·91	1·00
1173	60°	0·50	720	298	788	-0·23	0·8	466	713	0·64	2120	180	1·01	1·7	1440	418	0·38	1·01	1·72
1174	60°	0·48	975	1260	1470	-0·10	0·8	650	910	0·82	4680	644	0·81	1·7	1810	897	0·80	1·07	1·09
1175	60°	0·50	680	640	1160	0·07	0·8	680	835	0·75	3120	319	0·76	1·6	1060	572	0·51	0·82	1·19
1178	60°	0·43	1230	4340	3820	0·05	1·0	1230	1540	1·38	21700	1290	0·62	1·9	1820	1240	1·11	0·80	0·99

Notation

V = Estimated flutter speed – ft/sec

$$= \left(\frac{m_\theta}{\rho_0\, s c_m^2}\right)^{\frac{1}{2}} \frac{(0{\cdot}9-0{\cdot}33K)(1-0{\cdot}1r)\left(0{\cdot}95+\frac{1{\cdot}3}{\sigma_w}\right)\sec^{3/2}\left(\Lambda-\frac{\pi}{16}\right)}{0{\cdot}854\,(g-0{\cdot}1)(1{\cdot}3-h)}$$

$V_{A,B} = V\,(1{\cdot}3-h)$ – ft/sec

$M_{A,B} = \frac{V_{A,B}}{a_0}$ (a_0 = local speed of sound – ft/sec)

V_M = Measured flutter speed – ft/sec

G = Gravitational acceleration – ft/sec^2

K = Wing taper ratio $\left(=\frac{\text{tip chord}}{\text{root chord}}\right)$

c_m = Wing mean chord – ft

g = Distance of inertia axis aft of leading edge ÷ wing chord

h = Distance of flexural centre of loading section aft of leading edge ÷ wing chord

l_ϕ = Wing flexural stiffness measured at 0·7s – lb ft/rad

m_θ = Wing torsional stiffness measured at 0·7s – lb ft/rad

r = Stiffness ratio $\left(=\frac{l_\phi c_m^2}{0{\cdot}81\, m_\theta s^2}\right)$

s = Wing length from root to tip – ft

Λ = angle of sweepback

ρ_w = Wing density – slugs/ft^3 $\left(\frac{\text{Mass of one wing}}{s c_m^2}\right)$

ρ_0 = Air density at sea level – slugs/ft^3

σ_w = Wing relative density $\left(=\frac{\text{Wing density}}{\text{Air density}}\right)$

TABLE 4. Measured and Calculated Results

Model No	Λ	Measured Values: g	K_g	$\frac{W}{s}$	n_1	n_2	n_3	N	V	M	n	ω	$\frac{f}{G}$	V_F	Calculated Values: V_o	M_o	n_o	ω_o	$\frac{V}{V_o}$	$\frac{n}{n_o}$
1120	20°	0·45	0·28	1·44	16	76	84	0·42	675	0·60	29·0	0·29	35	820	603	0·54	45·5	0·50	1·12	0·64
1160	20°	0·42	0·26	1·70	37	122	190	0·45	1150	1·03	52·0	0·30	19	—	1010	0·90	74·0	0·49	1·04	0·70
1161*	20°	0·39	0·26	1·90	42	147	214	0·45	1275	1·14	54·0	0·28	47	—	1390	1·24	85·0	0·41	0·92	0·63
1162	20°	0·39	0·24	2·19	37	127	213	0·46	1160	1·04	58·0	0·33	19	—	1210	1·08	79·0	0·43	0·96	0·73
1163*	20°	0·40	0·25	1·92	45	150	250	0·44	1560	1·40	58·0	0·25	47	—	1350	1·21	85·0	0·42	1·15	0·68
1164	20°	0·42	0·25	2·02	32	73	162	0·47	725	0·65	35·5	0·33	27	980	615	0·55	48·0	0·52	1·18	0·74
1165	20°	0·45	0·28	1·50	12	73	74	0·47	Telemetry Failure					800	580	0·52	41·0	0·47	—	—
1166	20°	0·43	0·27	1·60	25	97	149	0·45	930	0·83	41·5	0·30	27	950	800	0·72	57·0	0·47	1·16	0·73
1167	20°	0·44	0·27	1·46	27	76	147	0·45	575	0·51	40·0	0·47	29	800	575	0·51	47·5	0·55	1·00	0·84
1124	40°	0·42	0·25	2·48	24	72	134	0·47	890	0·80	40·7	0·37	24	930	800	0·72	42·0	0·43	1·11	0·97
1125	40°	0·47	0·28	1·63	24	76	135	0·60	800	0·72	42·0	0·43	26	930	640	0·57	54·5	0·70	1·25	0·76
1129	40°	0·43	0·26	1·66	33	99	180	0·46	970	0·87	51·0	0·43	28	1090	925	0·83	62·0	0·55	1·05	0·82
1130	40°	0·43	0·29	1·99	23	88	118	0·49	1000	0·90	45·1	0·37	23	1220	826	0·74	60·0	0·60	1·21	0·75
1131	40°	0·45	0·28	1·58	9	59	59	0·39	530	0·47	27·2	0·42	24	650	596	0·53	34·5	0·48	0·89	0·79
1132	40°	0·47	0·28	1·63	24	76	135	0·60	790	0·71	37·0	0·38	20	870	640	0·57	54·5	0·70	1·25	0·68
1133	40°	0·43	0·27	1·90	21	63	118	0·47	650	0·58	32·7	0·41	22	840	640	0·57	40·0	0·51	1·02	0·82
1144*	40°	0·41	0·27	2·03	27	104	148	0·54	1125	1·01	54·8	0·40	43	1200	952	0·85	67·0	0·58	1·18	0·82
1145*	40°	0·42	0·27	2·15	29	102	157	0·48	1080	0·97	54·5	0·41	51	1340	950	0·85	66·0	0·57	1·14	0·83
1146*	40°	0·41	0·28	2·17	28	111	164	0·50	1120	1·00	55·0	0·40	50	—	1068	0·96	73·5	0·56	1·05	0·75
1147	40°	0·42	0·27	2·33	29	103	146	0·50	1270	1·14	52·0	0·34	14	—	1040	0·93	68·0	0·54	1·22	0·76
1148*	40°	0·40	0·26	2·51	32	125	178	0·49	No Flutter					—	1240	1·11	80·0	0·53	—	—
1149*	40°	0·40	0·26	2·56	35	130	180	0·50	No Flutter					—	1310	1·17	84·0	0·53	—	—
1150*	40°	0·42	0·28	2·40	32	106	164	0·47	1190	1·07	56·5	0·39	53	—	1260	1·13	63·5	0·41	0·94	0·89
1151*	40°	0·40	0·26	2·42	32	107	168	0·47	1160	1·04	53·1	0·38	54	—	1175	1·05	63·0	0·44	0·99	0·84
1152*	40°	0·40	0·26	2·52	32	112	182	0·50	1300	1·16	60·6	0·38	51	—	1110	0·99	73·0	0·52	1·17	0·84
1153*	40°	0·39	0·25	2·48	34	124	185	0·46	No Flutter					—	1510	1·35	71·0	0·39	—	—
1154*	40°	0·39	0·25	2·62	34	126	180	0·46	No Flutter					—	1490	1·33	69·0	0·38	—	—
1155	40°	0·39	2·25	2·64	14	60	84	0·48	780	0·70	27·3	0·29	22	930	612	0·55	36·5	0·49	1·27	0·75
1168*	60°	0·45	0·26	3·60	15	69	75	0·62	1020	0·91	34·5	0·38	37	1200	950	0·85	47·0	0·62	1·08	0·73
1169*	60°	0·44	0·26	3·91	18	63	84	0·58	1180	1·08	41·7	0·43	44	1425	910	0·81	46·0	0·63	1·30	0·91
1170*	60°	0·45	0·25	4·10	17	81	90	0·58	1330	1·19	52·0	0·45	39	1900	1190	1·07	56·0	0·59	1·12	0·93
1171*	60°	0·42	0·24	4·40	18	88	94	0·49	1580	1·41	49·0	0·35	39	2060	1360	1·22	51·0	0·47	1·16	0·96
1172*	60°	0·47	0·26	3·75	20	64	103	0·58	1135	1·02	37·6	0·41	47	1360	890	0·80	45·0	0·63	1·28	0·84
1173	60°	0·50	0·29	3·38	7	46	41	0·40	720	0·63	21·6	0·39	26	800	790	0·71	25·5	0·41	0·89	0·85
1174	60°	0·48	0·28	3·36	11	58	67	0·59	975	0·87	33·0	0·43	21	1050	825	0·74	41·0	0·62	1·18	0·81
1175	60°	0·50	0·28	3·17	10	48	55	0·56	680	0·61	25·0	0·40	24	820	630	0·56	33·0	0·66	1·08	0·76
1178*	60°	0·43	0·24	3·85	21	66	128	0·54	1230	1·10	45·0	0·46	47	—	955	0·86	40·0	0·53	1·29	1·12

Notation

Λ = angle of sweepback

g = distance of inertia axis aft of leading edge ÷ wing chord

K_g = radius of gyration of wing section about inertia axis ÷ wing chord

$\frac{W}{s}$ = wing weight per foot span — lb/ft

s = wing length root to tip, measured normal to root — ft

n_1 = fundamental flexure frequency — cycles/sec

n_2 = fundamental torsion frequency — cycles/sec

n_3 = overtone flexure frequency — cycles/sec

N = distance of nodal line for torsion mode aft of leading edge ÷ wing chord

V = measured flutter speed — ft/sec

M = measured Mach number

n = measured flutter frequency — cycles/sec

ω = measured flutter frequency parameter

$\frac{f}{G}$ = acceleration at flutter speed ÷ acceleration due to gravity

V_F = speed at wing failure — ft/sec

V_o = calculated flutter speed for incompressible flow — ft/sec

M_o = equivalent Mach number $\left(=\frac{V_o}{1117}\right)$

n_o = calculated flutter frequency — cycles/sec

ω_o = calculated flutter frequency parameter

Models marked thus* were tested using 5" rockets. All other models were tested using 3" rockets.

TABLE 5

Wing Data—Assumed Nodal Lines at 0·45c, 0·50c and 0·59c

Assumed N at 0·45c					Assumed N at 0·50c					Assumed N at 0·59c				
Model No.	Λ (deg)	N	g	K_G^2	Model No.	Λ (deg)	N	g	K_G^2	Model No.	Λ (deg)	N	g	K_G^2
1120	20	0·42	0·45	0·0784	1130	40	0·49	0·43	0·0841	1125	40	0·60	0·47	0·0784
1160	20	0·45	0·42	0·0676	1144	40	0·54	0·41	0·0729	1132	40	0·60	0·47	0·0784
1161	20	0·45	0·39	0·0676	1145	40	0·48	0·42	0·0729	1168	60	0·62	0·45	0·0676
1162	20	0·46	0·39	0·0576	1146	40	0·50	0·41	0·0784	1169	60	0·58	0·44	0·0676
1163	20	0·44	0·40	0·0625	1147	40	0·50	0·42	0·0729	1170	60	0·58	0·45	0·0625
1164	20	0·47	0·42	0·0625	1148	40	0·49	0·40	0·0676	1172	60	0·58	0·47	0·0676
1165	20	0·47	0·45	0·0784	1149	40	0·50	0·40	0·0676	1174	60	0·59	0·48	0·0784
1166	20	0·45	0·43	0·0729	1152	40	0·50	0·40	0·0676	1175	60	0·56	0·50	0·0784
1167	20	0·45	0·45	0·0729	1155	40	0·48	0·39	0·0625					
1124	40	0·47	0·42	0·0625	1171	60	0·49	0·42	0·0576					
1129	40	0·46	0·43	0·0676	1178	60	0·54	0·43	0·0576					
1131	40	0·38	0·45	0·0784										
1133	40	0·47	0·43	0·0729										
1150	40	0·47	0·42	0·0784										
1151	40	0·47	0·40	0·0676										
1153	40	0·46	0·39	0·0625										
1154	40	0·46	0·39	0·0625										
1173	60	0·39	0·50	0·0841										
Mean Values		0·449	0·424	0·0698	Mean Values		0·501	0·412	0·0692	Mean values		0·589	0·466	0·0724

Λ = Angle of sweepback
N = Distance of nodal line for torsion mode aft of leading edge ÷ wing chord
g = Distance of inertia axis aft of leading edge ÷ wing chord
K_G = Radius of gyration of wing section about inertia axis ÷ wing chord

TABLE 6

Calculated and measured flutter values for model 1178

	Flutter speed ft/sec	Flutter frequency cycles/sec	Frequency parameter
Assumed Modes ..	955	40·0	0·53
Measured Modes ..	920	39·5	0·54
Test Result ..	1230	45·0	0·46

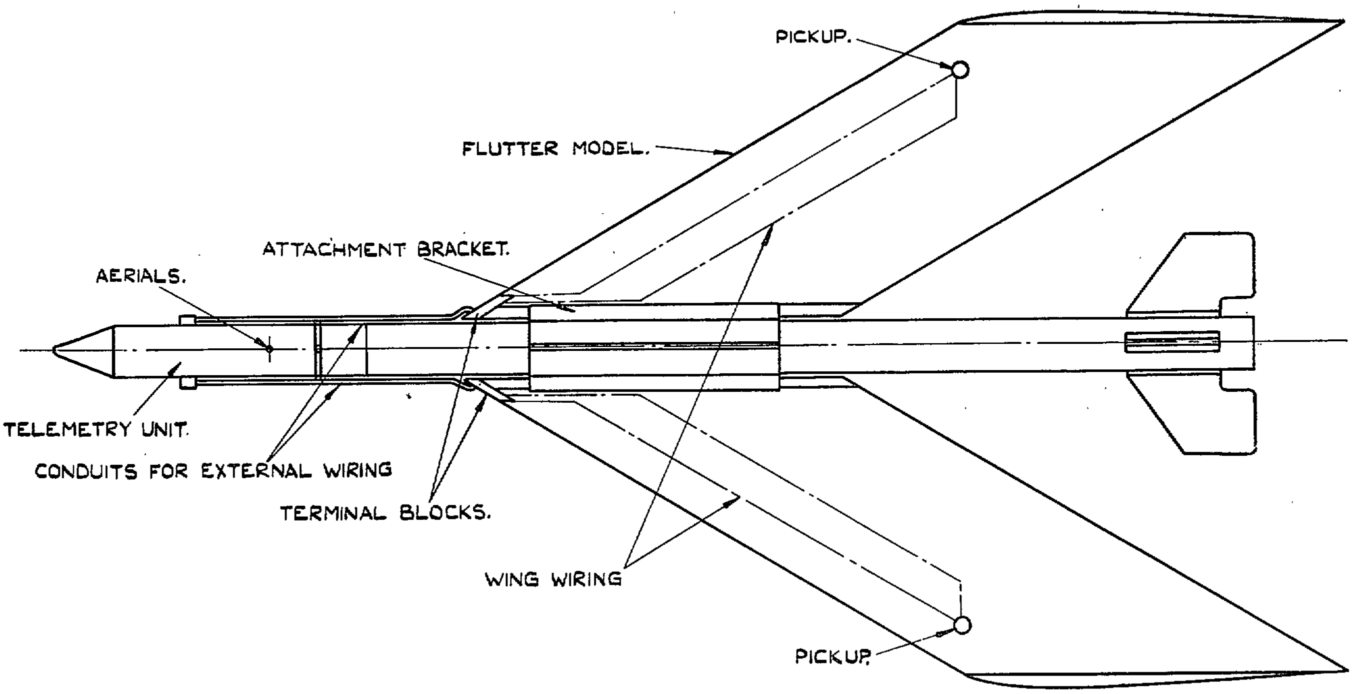

FIG. 1. Typical assembly, 3-in. rocket.

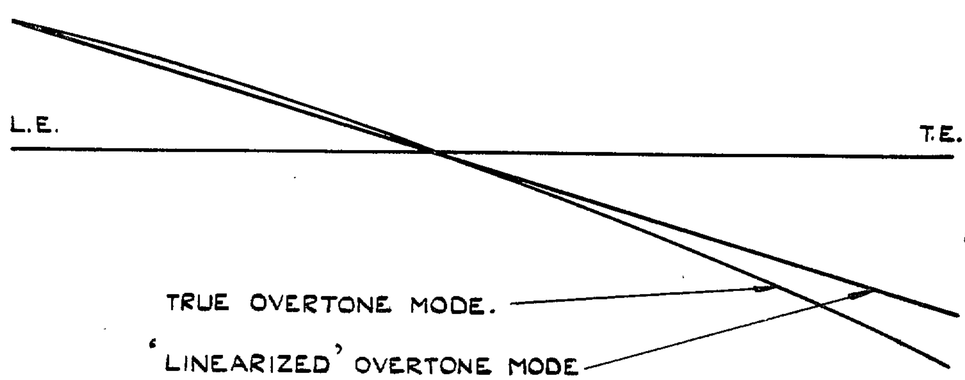

FIG. 2. Chordwise distortion of tip section in overtone vibration mode.

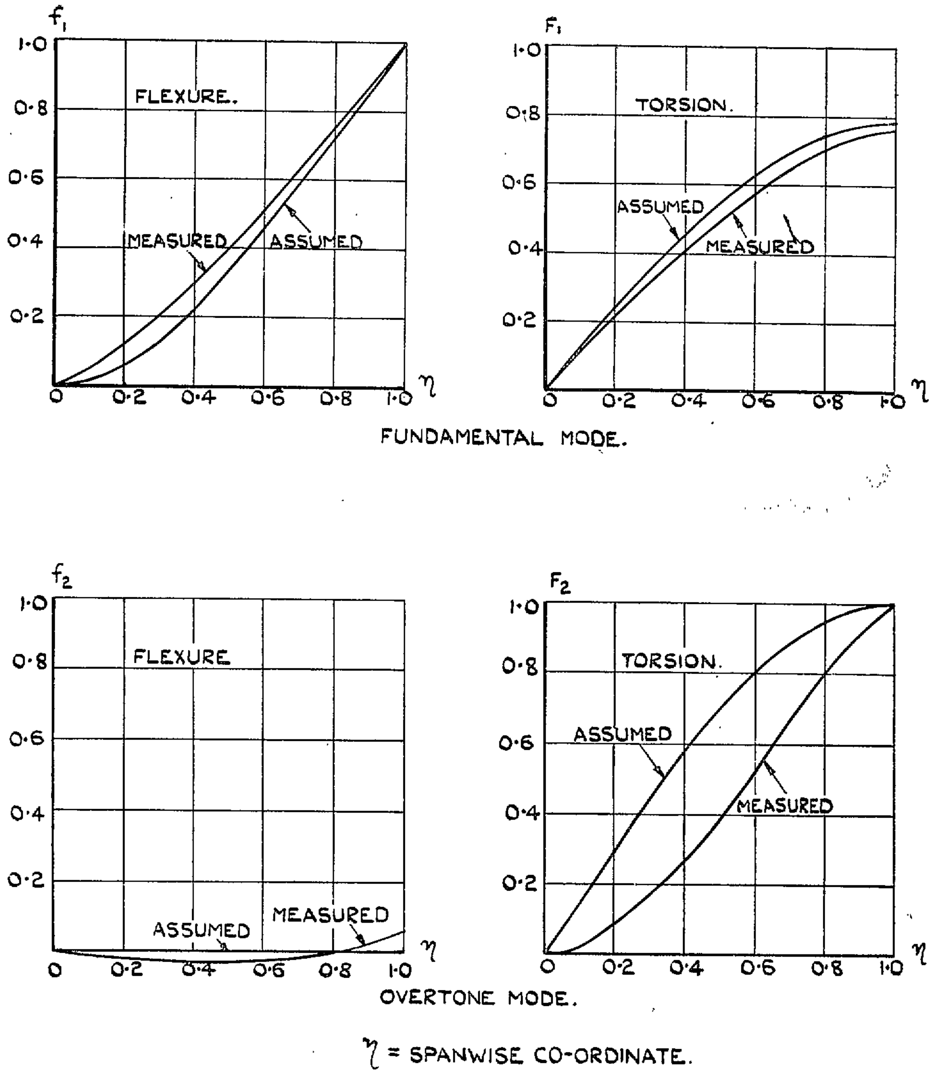

FIG. 3. Comparison of measured and assumed modes for model 1178.

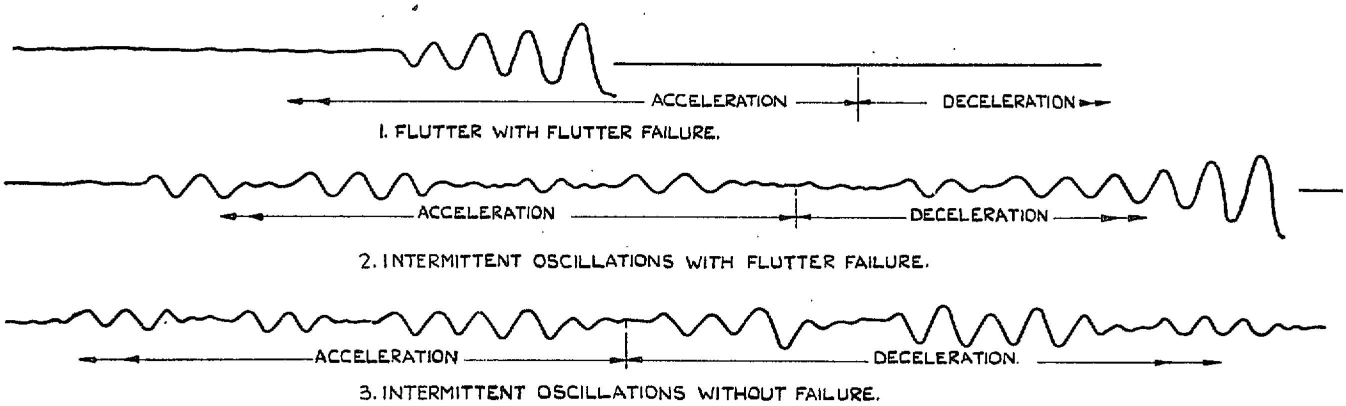

FIG. 4. Typical records of wing oscillations.

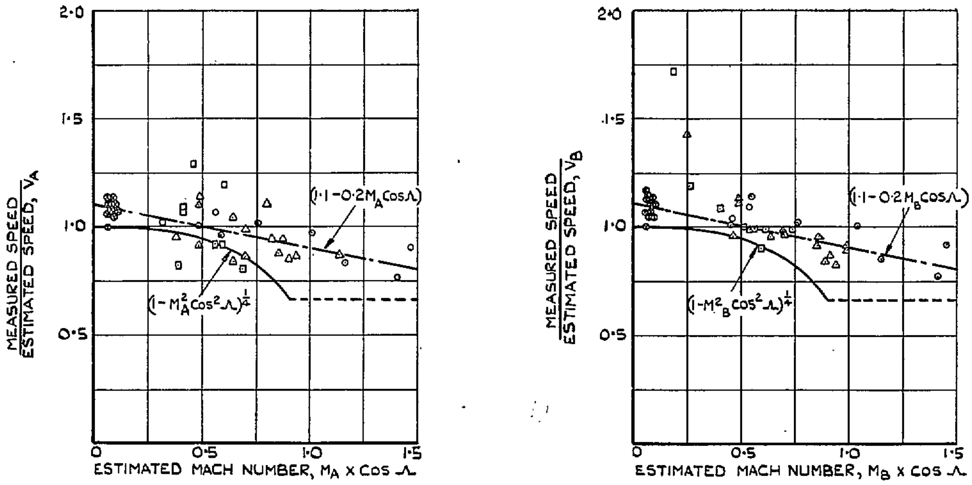

KEY	
SYMBOL	SWEEPBACK, Λ
⊙	20°
△	40°
⊡	60°
⊗	WIND TUNNEL MODELS

FIG. 5. Comparison of measured and estimated flutter speeds.

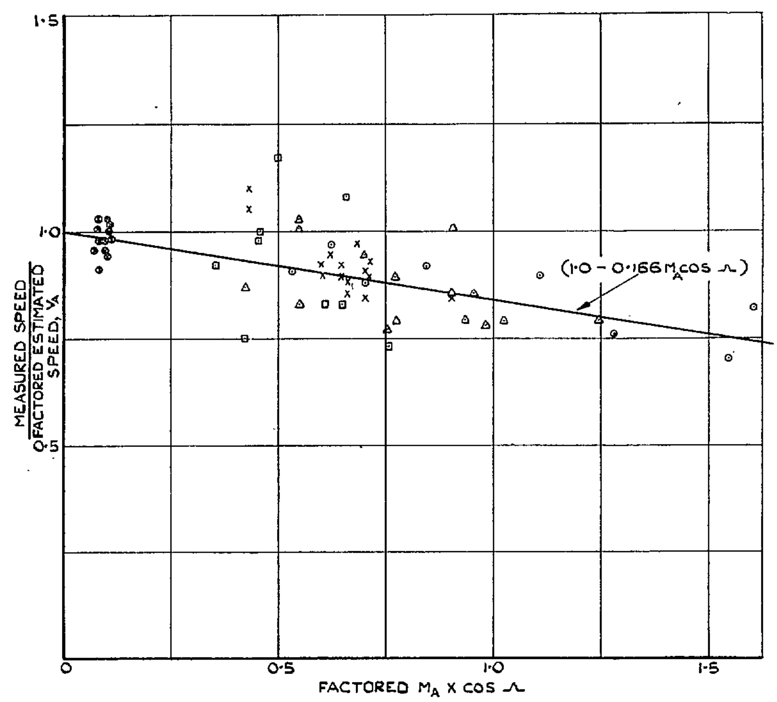

KEY	
SYMBOL	SWEEPBACK, Λ
×	0°
⊙	20°
△	40°
⊡	60°
⊗	WIND TUNNEL MODELS

FIG. 6. Comparison of measured and estimated flutter speeds, including results for unswept wings.

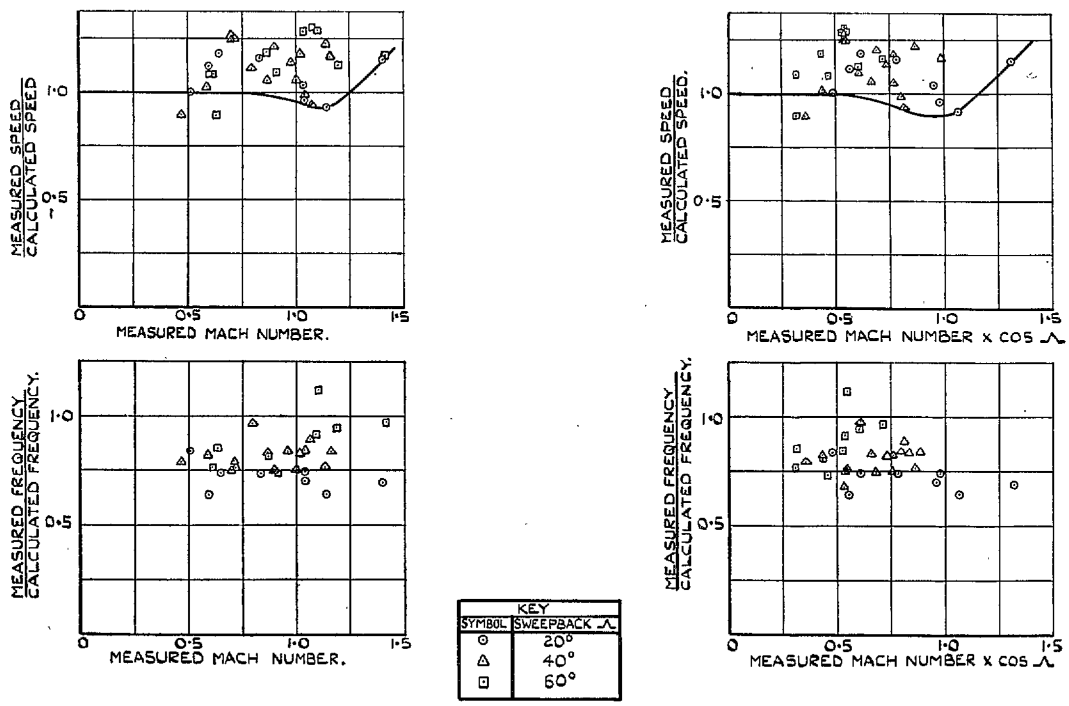

FIG. 7. Flutter speed and frequency rations plotted against Mach number at flutter.

(3835) Wt. 19/P.411 K.7 7/56 Hw. PRINTED IN GREAT BRITAIN